NANO LETTERS

Letter

pubs.acs.org/NanoLett

Surface Structured Optical Coatings with Near-Perfect Broadband and Wide-Angle Antireflective Properties

Emmett E. Perl,*[,†] William E. McMahon,[§] Robert M. Farrell,[‡] Steven P. DenBaars,[†,‡] James S. Speck,[‡] and John E. Bowers[†,‡]

[†]Department of Electrical and Computer Engineering and [‡]Materials Department, University of California, Santa Barbara, Santa Barbara, California 93106, United States

[§]National Renewable Energy Laboratory, Golden, Colorado 80401, United States

ABSTRACT: Optical thin-film coatings are typically limited to designs where the refractive index varies in only a single dimension. However, additional control over the propagation of incoming light is possible by structuring the other two dimensions. In this work, we demonstrate a three-dimensional surface structured optical coating that combines the principles of thin-film optical design with bio-inspired nanostructures to yield near-perfect antireflection. Using this hybrid approach, we attain average reflection losses of 0.2% on sapphire and 0.6% on gallium nitride for 300−1800 nm light. This performance is maintained to very wide incidence angles, achieving less than 1% reflection at all measured wavelengths out to 45° for sapphire. This hybrid design has the potential to significantly enhance the broadband and wide-angle properties for a number of optical systems that require high transparency.

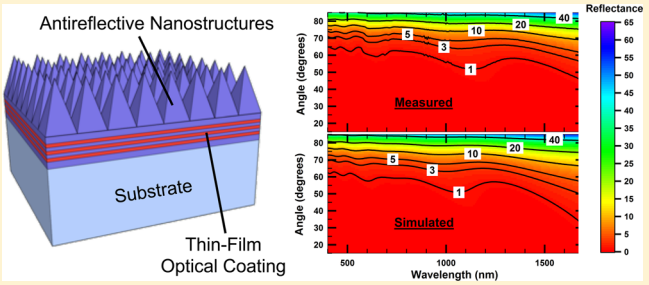

KEYWORDS: *Subwavelength structures, biomimetics, diffractive optics, thin films, antireflective nanostructures*

The principles of thin-film optics form the foundation for conventional optical coating design. This paradigm has enabled the development of a variety of optical elements, including high-reflectivity coatings, long-pass and short-pass filters, beam splitters, and antireflection filters.[1,2] While it is possible to make thin-film coatings of very high quality, most of these designs are one-dimensional in nature and do not allow for structural variation in the two lateral dimensions.[3]

There is another class of optical elements that utilize diffractive optics, which describes how light behaves when encountering an obstacle with a variable lateral structure.[4,5] When light is incident on a surface with periodic features, the transmitted beam can be split and diffracted to an angle, θ_T, which can be calculated using the grating equation

$$\sin(\theta_T) = \frac{m\lambda_0}{nd_{lat}} + \sin(\theta_I) \quad (1)$$

where m is the diffraction order, λ_0 is the wavelength of incoming light, n and d_{lat} are the refractive index and lateral spacing of the structure, and θ_I is the incidence angle. These principles are fundamental to the operation of diffraction gratings and have also led to the advent of antireflective nanostructures for the special case where only zeroth-order diffraction is possible ($m = 0$).[6] This condition is met when the lateral spacing of the structure satisfies the following:

$$d_{lat} < \left(\frac{\lambda_0}{n(1 - \sin(\theta_I))}\right) \quad (2)$$

Diffractive optics is essential to a number of photonic systems in which the propagation of light is controlled through surface structuring. However, diffractive optical elements typically do not employ the use of thin-film design.

By combining the principles of diffractive and thin-film optics, it is possible to attain additional control over the propagation of light.[7,8] We showed previously that transmission into a gallium arsenide-based four-junction solar cell can be dramatically increased using a hybrid design that combines surface structuring with a thin-film optical coating.[9,10] Here, we demonstrate near-perfect broadband and wide-angle antireflection for a hybrid design fabricated on gallium nitride and on sapphire.

These materials are technologically important for a number of applications that require high optical transparency. Because of its hardness (9 out of 10 on the Mohs hardness scale), sapphire is commonly used as the cover glass for camera lenses, watches, and other consumer electronics.[11] Gallium nitride has revolutionized solid-state lighting[12−14] and has demonstrated the potential to increase the efficiency of multijunction solar cells.[15−17] These technologies can benefit from improved broadband (~300−1800 nm for multijunction solar cells)[18] and wide-angle antireflection designs.

For thin-film coatings to attain high transmission for broadband and wide-angle light, it is necessary that the layers

Received: August 3, 2014
Revised: September 17, 2014
Published: September 19, 2014

   dx.doi.org/10.1021/nl502977f | *Nano Lett.* 2014, 14, 5960−5964

be composed of low-absorption materials that also span the refractive index range from air to the substrate.[10,19] Unfortunately, this is not always possible due to limitations in material availability. One limitation is that few solid materials exist with a refractive index lower than silicon dioxide ($n < 1.5$).[20] Importantly, this constraint leads to degradation in both the broadband and the wide-angle performance of any optical coating design. The second limitation is that there are not many low absorption materials with a refractive index higher than titanium dioxide ($n > 2.5$).[10,21] This primarily limits broadband transmittance into semiconductors with a high refractive index and is especially important for optical coatings on gallium arsenide-based multijunction solar cells.[9,10]

The first material constraint can be overcome using antireflective nanostructures that mimic the optical properties of a moth's eye.[6,22,23] These designs consist of nanoscale pyramids with subwavelength spacing and act to suppress all but zeroth-order diffraction.[6,24] When the lateral dimensions are sufficiently small, the structure can be modeled by splitting the nanopyramids into a large number of thin horizontal slices with an effective refractive index, n_{eff}, calculated using Bruggeman's effective medium approximation.[25] The symmetric 2-dimensional Bruggeman equation for two-material mixtures is[26,27]

$$0 = F\left(\frac{n_{\text{eff}} - n_1}{n_{\text{eff}} + n_1}\right) + (1 - F)\left(\frac{n_{\text{eff}} - n_0}{n_{\text{eff}} + n_0}\right) \quad (3)$$

where F is the areal fraction of the nanostructure material in each slice, n_0 is the refractive index of air, and n_1 is the refractive index of the nanostructure material. Reflectance off and transmittance through the nanostructures can then be calculated using the transfer-matrix method.

For nanopyramids, where F changes smoothly through the structure, incoming light will see a gradient in the effective index profile and will be partially reflected at each slice in the structure with a phase determined by the distance traveled through the material. For sufficiently tall nanostructures, all phases will be present in the reflected beam, and destructive interference will yield near-zero reflection for broadband and wide-angle light.[6,28]

The second constraint can be overcome by utilizing lower index ($n < 2.5$) materials in the substrate or active device. While most semiconductors have a very high refractive index ($n > 3$), both sapphire ($n \approx 1.8$) and gallium nitride ($n \approx 2.4$) have a refractive index comparable to the transparent materials used for thin-film optical coating design.[29]

Our surface structured optical coating operates by combining nanostructures, which reduce reflection from air to silicon dioxide (SiO_2), with a multilayer optical coating, which is optimized for minimum reflection from SiO_2 to the substrate. When this hybrid design is applied to sapphire or gallium nitride, both material constraints are eliminated and near-perfect broadband and wide-angle antireflection is possible.

Figure 1 shows various illustrations of the surface structured optical coating, where the scanning electron micrograph (SEM) and atomic force microscope (AFM) profile are taken for a design placed onto a single side polished (SSP) sapphire substrate. Figure 1a,c shows a three-dimensional diagram of the design and its corresponding refractive index profile. The SEM cross-section and AFM profile from Figure 1b,d allow us to approximate the nanostructure dimensions and the refractive

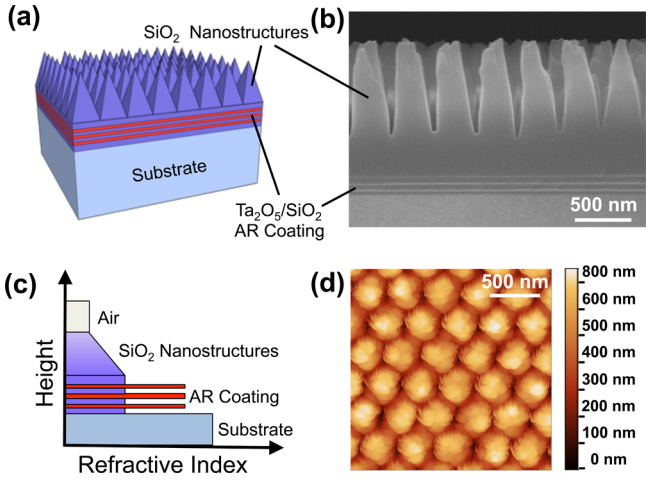

Figure 1. Illustration of the surface structured optical coating showing (a) a three-dimensional diagram of the hybrid design, (b) a cross-sectional SEM of the hybrid design placed onto sapphire, (c) the refractive index profile of the design, and (d) a two-dimensional profile of the antireflective nanostructures measured using AFM.

index profile for the hybrid design. The nanostructure height and pitch are approximately 800 and 350 nm, respectively.

The first fabrication step is to design and deposit a multilayer optical coating on the surface of the sample. We limit ourselves to designs consisting of alternating layers of tantalum pentoxide (Ta_2O_5) and SiO_2. These materials are chosen because they absorb minimal 300−1800 nm light and can be combined to form Herpin pairs with the equivalent optical properties of an intermediate index material.[10,19,30,31] This enables these designs to achieve near-optimal performance by spanning the entire refractive index range from SiO_2 to sapphire and most of the range from SiO_2 to gallium nitride. To optimize the layer thicknesses, we perform a global search and then minimize reflectance for 300−1800 nm light using a simplex optimization.[9,10]

The multilayer coatings are deposited using a VEECO ion-beam-assisted sputter deposition system. After deposition of the multilayer coating, a thick (≈1.5 μm) layer of SiO_2 is placed onto the sample. This is followed by a nanoimprinting process and dry etching step to transfer the antireflective nanostructures from a master stamp to the SiO_2 layer. Additional details on the fabrication process are reported elsewhere.[9]

Figure 1b shows a cross-sectional SEM of the completed hybrid design. While the nanostructures appear coarse, it is important to note that this roughness occurs on a scale that is much smaller than the wavelength of the light that we are considering (300−1800 nm) and should not contribute significantly to scattering.[6,10,32] It is also evident that there is a SiO_2 buffer of approximately 300 nm between the uppermost Ta_2O_5 layer and the bottom of the nanostructures. It is important to include this buffer layer in the optical model when simulating these designs.

Figure 1d shows a two-dimensional profile of the nanostructures measured on a VEECO Dimension 3100 AFM with high aspect ratio AFM tips that are 2 μm tall. With this profile, we can extract the areal fraction, F, of SiO_2 for a large number of thin horizontal slices. These data are input into eq 3 and used to calculate the refractive index profile for the fabricated hybrid designs. The nanostructures are modeled using a 140-slice approximation, which we previously showed is

dx.doi.org/10.1021/nl502977f | Nano Lett. 2014, 14, 5960−5964

a very accurate representation of the optical properties for the nanostructure layer.[10]

Figure 2 shows the measured and simulated reflectance for SSP sapphire and gallium nitride samples with an optimal hybrid antireflection design, a multilayer antireflection coating, and no optical coating. Specular reflectance is measured at an incidence angle of 8° using a Cary 500 UV−Vis−NIR spectrophotometer. Black paint is placed onto the roughened backside of the samples to minimize unwanted reflections from the unpolished surface.

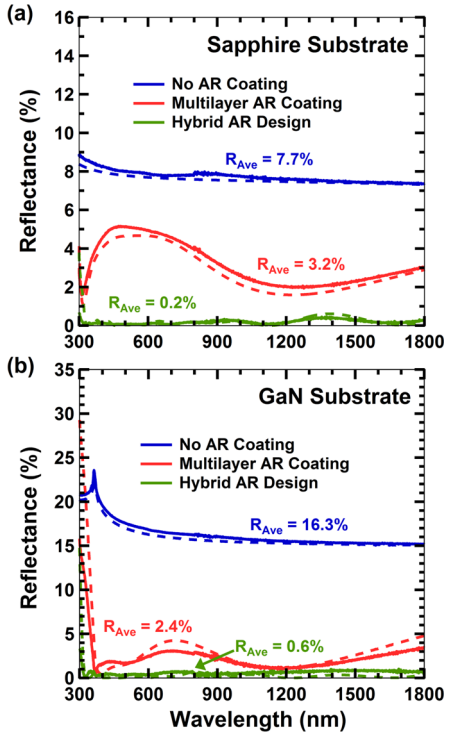

Figure 2. Plot of the simulated (dashed lines) and measured (solid lines) reflectance spectrum showing the broadband performance of a hybrid AR design and an optimal multilayer AR coating for (a) sapphire and (b) gallium nitride.

It is evident that the hybrid design can outperform a conventional multilayer antireflection coating. For 300−1800 nm light, the average measured reflectance of the surface structured optical coating is just 0.2% for the design placed on sapphire and 0.6% for the design placed on gallium nitride. This represents a 16× decrease in broadband reflectance for sapphire and 4× decrease for gallium nitride compared to an optimized thin-film antireflection coating.

The hybrid design also maintains its quality to very wide incidence angles. Contour plots showing reflectance as a function of both angle and wavelength are shown in Figure 3 for the hybrid design and multilayer antireflection coating on SSP sapphire. Reflectance is measured using a V-VASE ellipsometer for incidence angles between 15° and 85°. The values shown are averaged from the s- and p-polarization components of light.

We measure less than 1% reflectance at all wavelengths out to an angle of 45° for the hybrid design. In comparison, the reflectance of the multilayer antireflection coating does not drop below 1% for any wavelength or angle measured. The hybrid design achieves much better wide-angle performance than a conventional multilayer AR coating for a couple reasons. First, the nanostructure layer has excellent wide-angle antireflective properties due to its smoothly varying refractive index profile.[6,28] Since light is partially reflected at every point in the structure, destructive interference will be maintained even at wide incidence angles. Second, wide-angle light will be bent closer to normal incidence in SiO_2 due to Snell's law of refraction, and the magnitude of the partial reflections at the thin-film interfaces will not increase as rapidly as they would for the air−SiO_2 interface.

We also note that there is excellent agreement between the measured and simulated reflectance for both designs. This suggests that our model accurately describes the optical properties of the nanostructures, and also provides indirect evidence that the nanostructure layer is not scattering or diffracting a significant amount of light.[9]

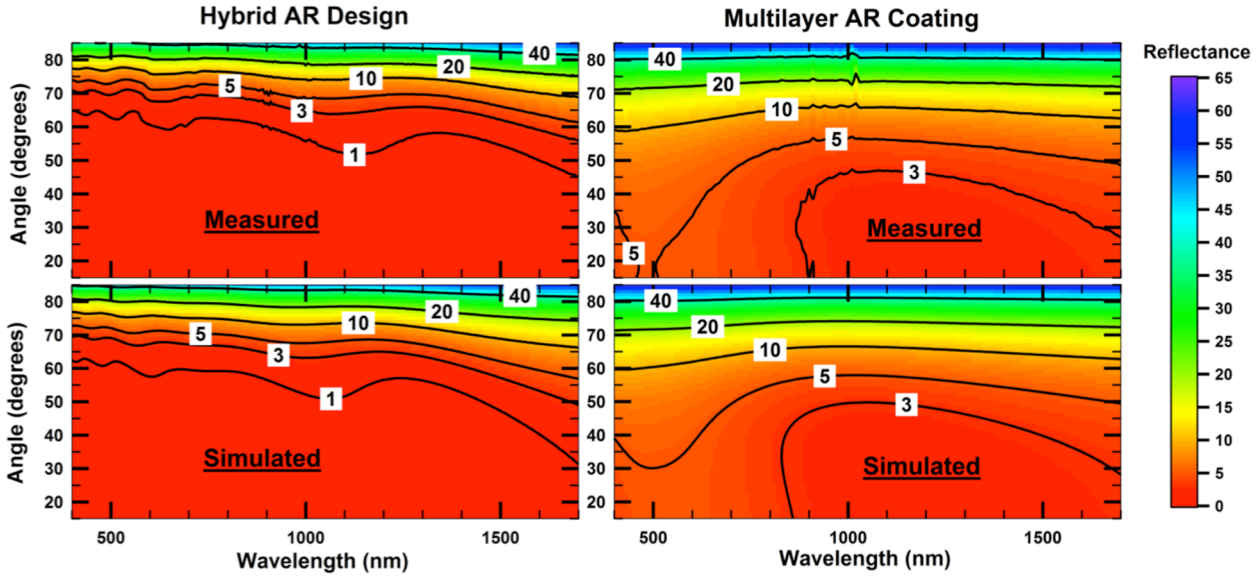

Figure 3. Contour plots showing simulated and measured reflectance as a function of both angle and wavelength for the optimal hybrid AR design (left) and multilayer AR coating (right).

dx.doi.org/10.1021/nl502977f | *Nano Lett.* 2014, 14, 5960−5964

To further investigate scattering and diffraction in the nanostructures, we measure reflectance and transmittance for a double side polished (DSP) sapphire sample with a hybrid design placed on both surfaces. These measurements are shown in Figure 4, where loss from absorption, scattering, and

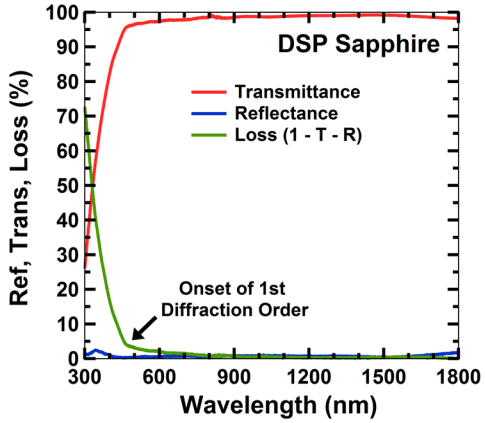

Figure 4. Plot showing reflectance, transmittance, and optical loss ($1 - T - R$) for a hybrid AR design placed on both sides of a DSP sapphire sample. Optical losses can be attributed to absorption, scattering, and diffraction.

diffraction can be quantified as the amount of light that is not specularly reflected or transmitted through the structure ($1 - T - R$).

These optical losses are very small for most of the wavelengths considered, averaging just 0.7% for 500−1800 nm light. However, we observe a large increase in optical loss between 450 and 500 nm. This wavelength range corresponds to the onset of the first diffraction order, which occurs when eq 2 is no longer satisfied. To attain higher transmittance between 300 and 500 nm, it is necessary to further reduce the lateral dimensions of the nanostructures. It is important to emphasize that both scattering and diffraction loss are minimized when the nanostructures are composed of materials with a low refractive index, such as SiO_2. For this reason, we expect that our hybrid design will have lower optical losses than antireflective nanostructures placed directly into the substrate material.

For simplicity, all of the hybrid designs in this study were fabricated on single material substrates. However, additional considerations must be taken into account when placing the hybrid design onto optoelectronic devices such as LED's or multijunction photovoltaics. These devices usually have surface topology, such as grids and mesas, which can make nanoimprinting difficult. One solution is to use soft nanoimprint lithography, which utilizes flexible stamps that can successfully imprint onto nonplanar samples.[33] Another consideration is that the epitaxial structure of these devices typically consist of many different semiconductor layers. However, it is important to note that the index contrast between these layers is typically small and usually will not have a major effect on the design of the thin-film optical coating.[9,10,16]

In conclusion, our results indicate that it is possible to significantly decrease reflection for broadband and wide-angle light using a design that integrates antireflective nanostructures with a multilayer optical coating. These hybrid designs attain a reflectance of 0.2% on sapphire and 0.6% on gallium nitride for 300−1800 nm light. Moreover, these broadband antireflective properties are maintained to wide incidence angles. For the hybrid design on sapphire, we measure less than 1% reflection loss across all measured wavelengths out to an incidence angle of 45°. To quantify scattering and diffraction losses, we measure reflection and transmission for a hybrid design placed on a DSP sapphire sample. We find an average optical loss of 0.7% for 500−1800 nm light, suggesting that scattering and diffraction are minimal at these wavelengths. However, scattering and diffraction increase significantly at shorter wavelengths where the onset of first-order diffraction occurs. Overall, this hybrid strategy has the potential to markedly enhance the broadband and wide-angle properties for optical systems that require low reflection and high transparency.

AUTHOR INFORMATION

Corresponding Author

*E-mail: emmettperl@ece.ucsb.edu (E.E.P.).

Notes

The authors declare no competing financial interest.

ACKNOWLEDGMENTS

This material is based upon work supported by the Center for Energy Efficient Materials, an Energy Frontier Research Center funded by the U.S. Department of Energy, Office of Science, Office of Basic Energy Sciences, under Award DE-SC0001009. A portion of this work was done in the UCSB nanofabrication facility, part of the NSF NNIN network (ECS-0335765). The sapphire substrates used for this study were provided by Namiki Precision Jewel. Emmett E. Perl is supported by the National Science Foundation Graduate Research Fellowship under Grant DGE-1144085.

REFERENCES

(1) Epstein, L. I. *J. Opt. Soc. Am.* **1952**, *42*, 806−808.
(2) Macleod, H. A. *Thin-Film Optical Filters*; CRC Press: Boca Raton, FL, 2001.
(3) Tikhonravov, A. V. *Appl. Opt.* **1993**, *32*, 5417−5426.
(4) Hutley, M. C. *Diffraction Gratings (Techniques of Physics)*; Academic Press: London, 1982.
(5) Suleski, T. J.; Kathman, A. D.; Prather, D. W. *Diffractive Optics: Design, Fabrication, and Test*; SPIE Press: Bellingham, WA, 2004.
(6) Wilson, S. J.; Hutley, M. C. *J. Mod. Opt.* **1982**, *29*, 993−1009.
(7) Yablonovitch, E. *J. Opt. Soc. Am. B* **1993**, *10*, 283−295.
(8) Lalanne, P.; Hutley, M. C. *Encyclopedia of Optical Engineering*; CRC Press: Boca Raton, FL, 2003; pp 62−71.
(9) Perl, E. E.; Lin, C.-T.; McMahon, W. E.; Friedman, D. J.; Bowers, J. E. *IEEE J. Photovoltaics* **2014**, *4*, 962−967.
(10) Perl, E. E.; McMahon, W. E.; Bowers, J. E.; Friedman, D. J. *Opt. Express* **2014**, *22*, A1243−A1256.
(11) Christoph, R. *Laser Technol. J.* **2014**, *11*, 48−50.
(12) Nakamura, S.; Senoh, M.; Iwasa, N.; Nagahama, S.-I. *Jpn. J. Appl. Phys.* **1995**, *34*, L797−L799.
(13) Pimputkar, S.; Speck, J. S.; DenBaars, S. P.; Nakamura, S. *Nat. Photonics* **2009**, *3*, 180−182.
(14) Schubert, E. F.; Gessmann, T.; Kim, J. K. *Light Emitting Diodes*; Cambridge University Press: Cambridge, 2006.
(15) Matioli, E.; Neufeld, C.; Iza, M.; Cruz, S. C.; Al-Heji, A. A.; Chen, X.; Farrell, R. M.; Keller, S.; DenBaars, S.; Mishra, U.; Nakamura, S.; Speck, J.; Weisbuch, C. *Appl. Phys. Lett.* **2011**, *98*, 021102.
(16) Young, N. G.; Perl, E. E.; Farrell, R. M.; Iza, M.; Keller, S.; Bowers, J. E.; Nakamura, S.; DenBaars, S. P.; Speck, J. S. *Appl. Phys. Lett.* **2014**, *104*, 163902.
(17) McMahon, W. E.; Lin, C.-T.; Ward, J. S.; Geisz, J. F.; Wanlass, M. W.; Carapella, J. J.; Olavarría, W.; Young, M.; Steiner, M. A.;

France, R. M.; Kibbler, A. E.; Duda, A.; Olson, J. M.; Perl, E. E.; Friedman, D. J.; Bowers, J. E. *IEEE J. Photovoltics* **2013**, *2*, 868−872.
(18) Friedman, D. J.; Olson, J. M.; Kurtz, S. R. High-efficiency III-V multijunction solar cells. In *Handbook of Photovoltaic Science and Engineering*, 2nd ed.; Luque, A., Hegedus, S., Eds.; Wiley: Chichester, UK, 2011; pp 314−364.
(19) Aiken, D. J. *Sol. Energy Mater. Sol. Cells* **2000**, *64*, 393−404.
(20) Xi, J. Q.; Schubert, M. F.; Kim, J. K.; Schubert, E. F.; Chen, M.; Lin, S.-Y.; Liu, W.; Smart, J. A. *Nat. Photonics* **2007**, *1*, 176−179.
(21) Herve, P.; Vandamme, L. K. J. *Infrared Phys. Technol.* **1994**, *35*, 609−615.
(22) Bernhard, C. G. *Endeavor* **1967**, *26*, 79−84.
(23) Wilson, S. J.; Hutley, M. C. *J. Mod. Opt.* **1982**, *29*, 993−1009.
(24) Stavroulakis, P. I.; Boden, S. A.; Johnson, T.; Bagnall, D. M. *Opt. Express* **2013**, *21*, 1−11.
(25) Stavenga, D. G.; Foletti, S.; Palasantzas, G.; Arikawa, K. *Proc. R. Soc. London, Ser. B* **2006**, *273*, 661−667.
(26) Zhang, D. *Inverse Electromagnetic Problem for Microstructured Media*; Proquest: Ann Arbor, MI, 2007.
(27) Garahan, A.; Pilon, L.; Yin, J. *J. Appl. Phys.* **2007**, *101*, 014320.
(28) Southwell, W. H. *Opt. Lett.* **1983**, *8*, 584.
(29) Polyanskiy, M. N. Refractive Index Database, 2014; http://refractiveindex.info.
(30) Southwell, W. *Appl. Opt.* **1985**, *24*, 457−460.
(31) Victoria, M.; Domínguez, C.; Antón, I.; Sala, G. *Opt. Express* **2012**, *20*, 8136−8147.
(32) Hobbs, D. S.; MacLeod, B. D.; Riccobono, J. R. *Proc. SPIE* **2007**, *6545*, 65450Y.
(33) Viheriälä, J.; Tommila, J.; Leinonen, T.; Dumitrescu, M.; Toikkanen, L.; Niemi, T.; Pessa, M. *Microelectron. Eng.* **2009**, *86*, 321−324.